TID2026–011

The 18.6-year Lunar Nodal Cycle in Internal Tides

Zhongxiang Zhao[1,2], Chenxuan Ji[3], J. A. Mattias Green[4], and Richard Ray[5]

1 Applied Physics Laboratory, University of Washington, Seattle, Washington, USA. 2 School of Oceanography, University of Washington, Seattle, Washington, USA. 3 Astrophysics Group, Imperial College London, London, UK. 4 School of Ocean Sciences, Bangor University, Menai Bridge, UK. 5 NASA Goddard Space Flight Center, Greenbelt, Maryland, USA.

Introduction

The 18.6-year lunar nodal cycle (LNC) is caused by the Moon's time-varying declination ranging 18.3°--28.6°. It modulates the Earth's tidal potential and the amplitudes and phases of all lunar tidal constituents. The LNC can be expressed the form of $f(t)\,A\cos(\omega t + \phi + u(t))$, where A, ω, and ϕ are the amplitude, frequency, and phase of the tidal constituent, and $f(t)$ and $u(t)$ denote the small adjustments on amplitude and phase. **Table 1** lists the equilibrium-based amplitude factors and phase shifts. The LNC is known to impact extreme sea levels, coastal floods, and marine ecosystems. However, its modulation of internal tides has not been explored yet. Here, we demonstrate that (1) the LNC is detected in internal tides as expected by the equilibrium tide theory, and (2) the LNC can modulates the global distribution of internal tidal energy and thus affects ocean circulations and global climate.

Table 1. The 18.6-year Nodal Modulation for Six Lunar Constituents.

Tide	Amplitude factor f	Phase shift u
O_1, Q_1	$1.009 + 0.187\cos N - 0.015\cos 2N$	$10.8° \sin N - 1.3° \sin 2N$
K_1	$1.006 + 0.115\cos N - 0.009\cos 2N$	$-8.9° \sin N + 0.7° \sin 2N$
M_2, N_2	$1.000 - 0.037\cos N$	$-2.1° \sin N$
K_2	$1.024 + 0.286\cos N + 0.008\cos 2N$	$-17.7° \sin N + 0.7° \sin 2N$

Data

It is very challenging to extract the weak LNC signal in internal tides from a noisy ocean. Here we map internal tides using 30 years of satellite altimetry sea-surface height (SSH) measurements from 1993 to 2022 (**Figure 1a**). We divide the data into 28 overlapping subsets of equal size (**Figure 1b**). Each subset is approximately 12 satellite-years long; therefore, the resulting internal tide fields have almost the same error levels.

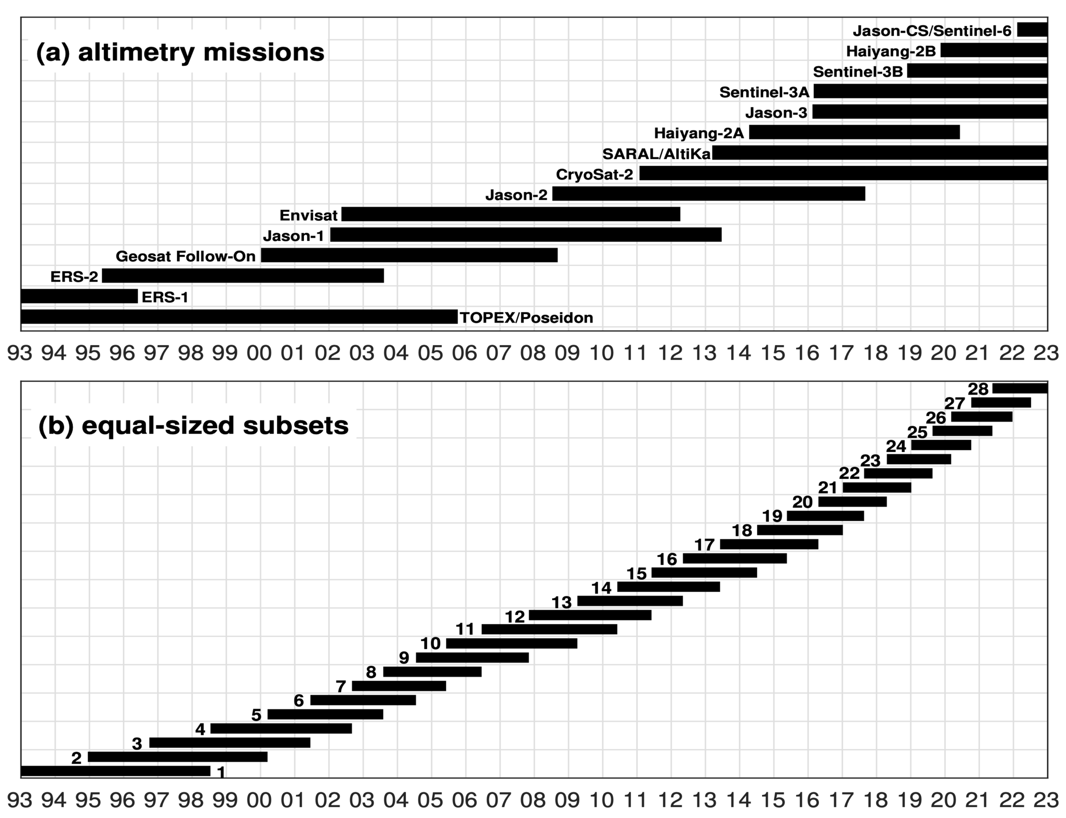

Figure 1. Satellite altimetry data. (a) 15 nadir-looking altimetry missions from 1993 to 2022. (b) 28 equal-sized subsets. The total data record is 120 satellite-years long. Each subset is 12 satellite-years long.

Methods

We map internal tides following our recently improved 3-step procedure that consists of two rounds of plane wave analysis with a spatial bandpass filter in between. For each subset, we map one set of global internal tide fields for mode-1 K_1, O_1, and M_2. Their 30-year coherent fields are obtained by averaging their 28 fields, respectively. As an example, **Figure 2** shows the #1, #28, and 30-year K_1 internal tide fields. The #1 and #28 fields are separated by about 26 years and show the largest interannual changes. These IT maps are done without any prior adjustment for the LNC.

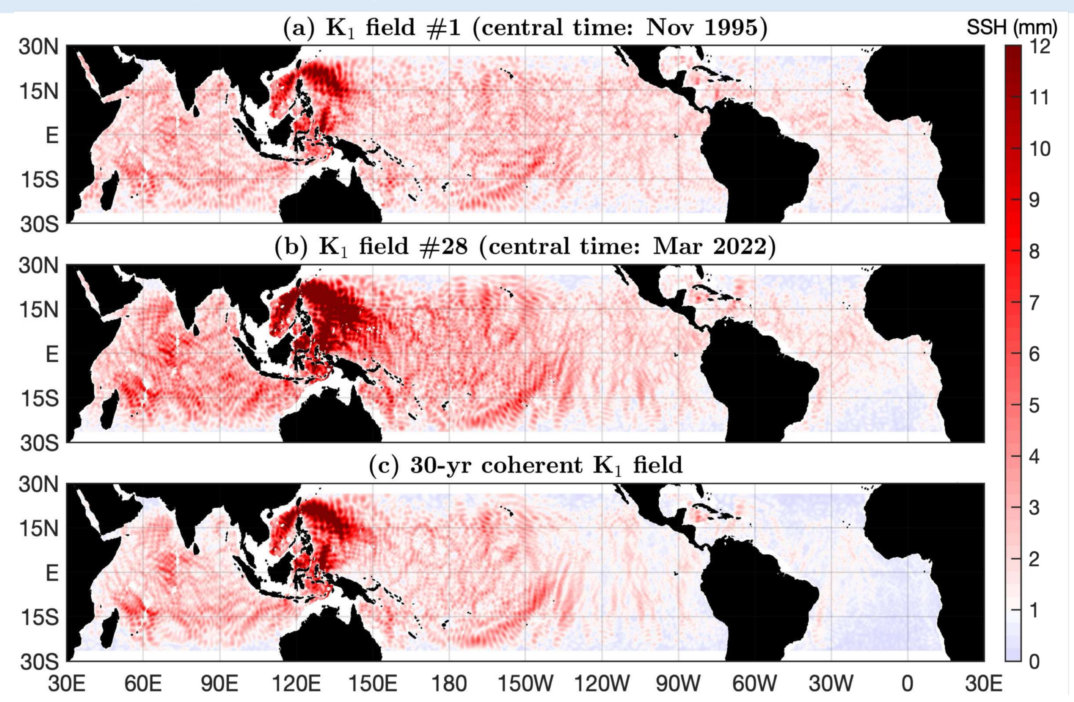

Figure 2. Global mode-1 K_1 internal tide fields from the total and subsetted satellite altimetry data.

Contrasting Internal Tide Fields

Figure 3 shows the density scatter plots for six pairs of fields as labeled. For each constituent, its internal tide fields all have a tight linear relation. They demonstrate significant interannual variability: the #1 fields are 0.70 (K_1) and 0.55 (O_1) of their 30-year fields; the #28 fields are 1.43 (K_1) and 1.56 (O_1) of their 30-year fields. Analyses of all 28 field reveal that the amplitude ratios are dominated by the 18.6-year LNC and 30-year trends.

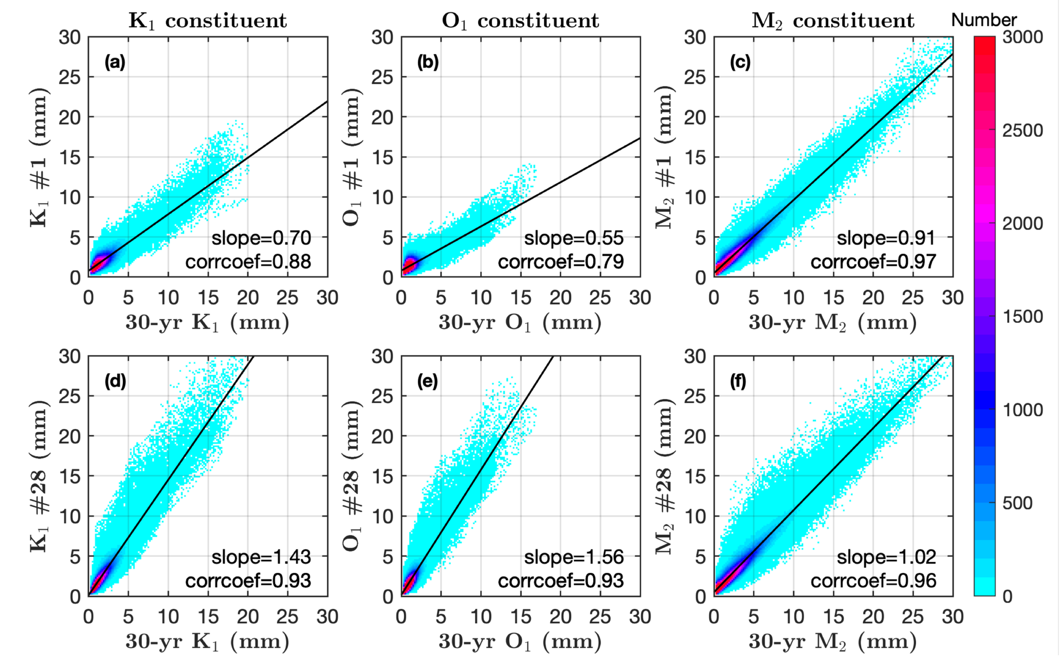

Figure 3. Density scatter plots of six pairs of internal tide fields as labeled. Color shading shows the number of points in 0.2 mm by 0.2 mm bins.

Pointwise Amplitude Factors

We obtain a time series of 28 amplitude ratios at each grid point. We fit the time series using the theoretical 18.6-year LNC given in **Table 1**. **Figure 4** shows the fitted amplitude factors of the 18.6-year LNC using pointwise amplitude ratios (see **Figure 3**). The global means of their amplitude factors are 0.121 (K_1), 0.169 (O_1), and 0.027 (M_2), respectively, consistent with their theoretical values based on the equilibrium tide theory.

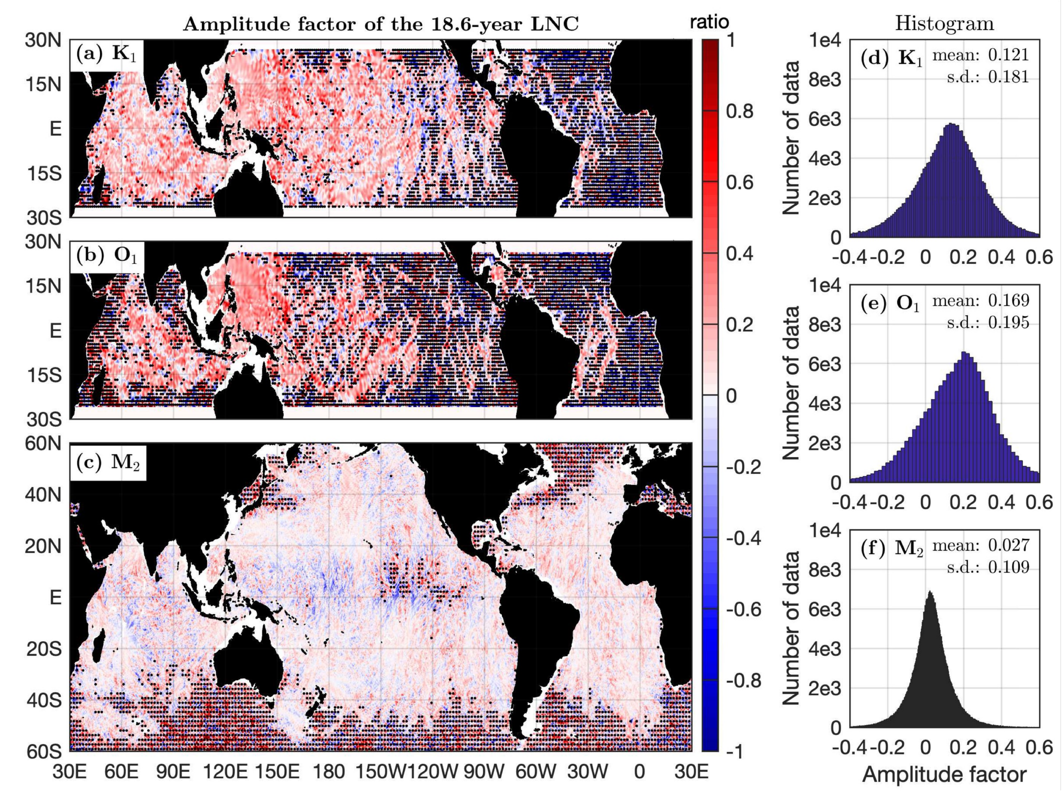

Figure 4. (a)-(c) Pointwise amplitude factors of the 18.6-year LNC. Internal tides with amplitudes <1 mm are hatched. (d)-(f) Histograms for internal tides with amplitudes >1 mm.

30-year Trends

We calculate global-mean amplitudes and phases for each constituent (**Figure 5**). Internal tides with amplitudes <1 mm are excluded. The six amplitude and phase time series all are dominated by two outstanding components: 18.6-year cycles and 30-year trends. The increases in amplitude and propagation speed are consistent with enhanced stratification with global ocean warming over the past 30 years. The 18.6-year LNC is consistent with the equilibrium tide theory.

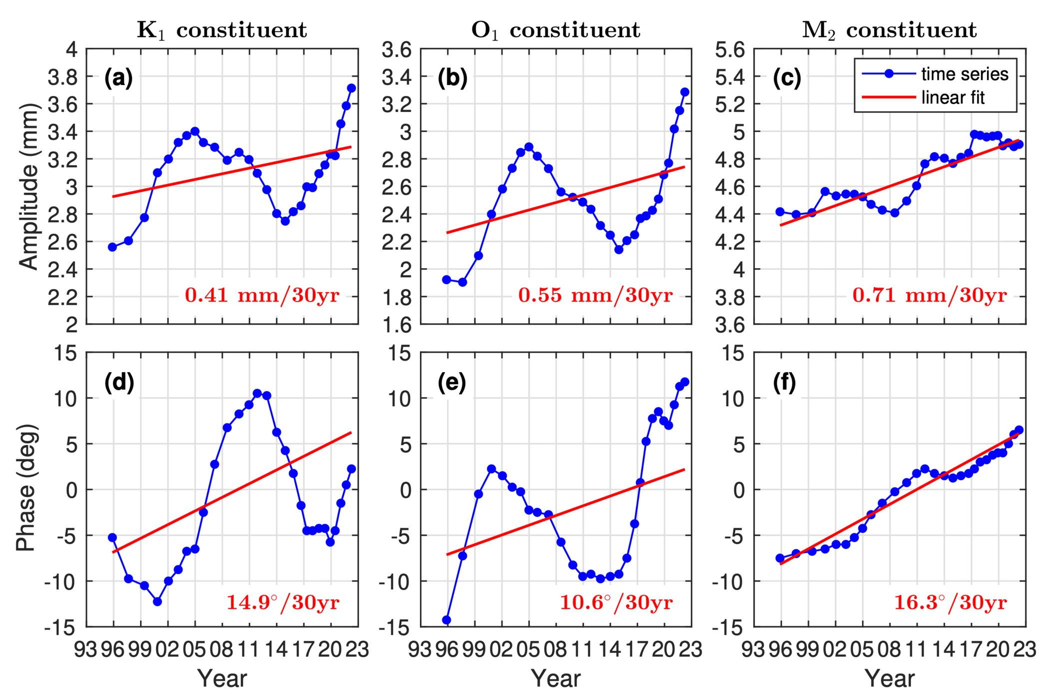

Figure 5. Global-mean amplitude and phase time series. All are dominated by 30-year trends (red lines) and 18.6-year cycles.

Nodal Modulation of IT Energy

The 18.6-year LNC can modulate the global distribution of internal-tide energy. In the time domain, K_1 and O_1 are 180° out of phase with M_2 in the cycle. In the space domain, these internal tidal constituents have very different spatial patterns. **Figure 6** shows the nodal modulation of the global distribution of internal-tidal energy. Here the depth-integrated internal tide energy is computed from SSH amplitudes and transfer functions.

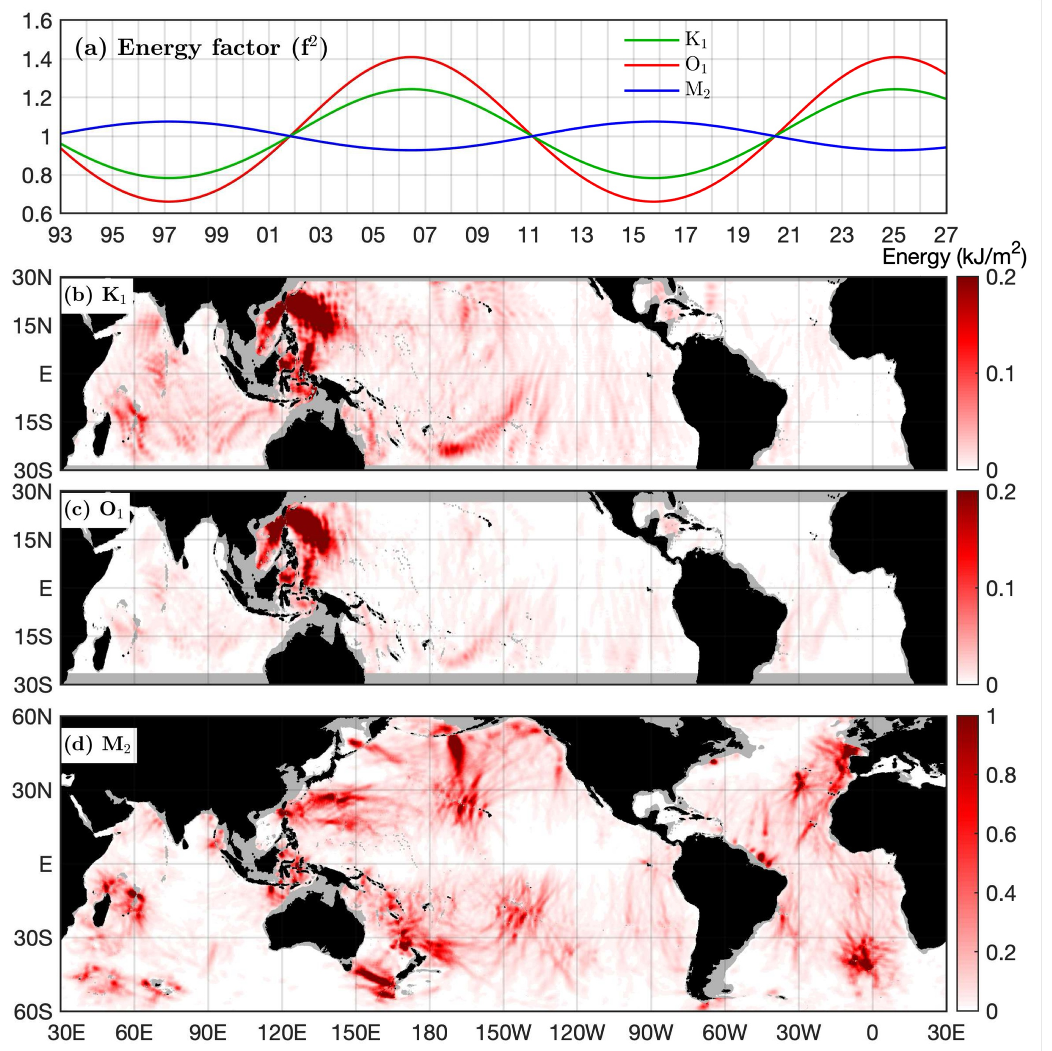

Figure 6. Nodal modulation on internal tidal energy. (a) The energy factor. (b)-(d) The 30-year coherent K_1, O_1, and M_2 internal-tide energy densities, in kJ / m^2.

Figure 7 shows the summed internal tide energy and variability. There are two contrast regions: Around the Luzon Strait, internal tidal energy is dominated by K_1 and O_1, because the diurnal constituents are stronger than the semidiurnal M_2 constituent. At high latitudes and in the Atlantic Ocean, internal tidal energy is mainly modulated by M_2, because there are no K_1 and O_1 at latitudes beyond 30° and very weak K_1 and O_1 in the Atlantic Ocean.

It is well known that the geography of internal wave-driven mixing significantly affects the global large-scale circulations. Given that the 18.6-year LNC can modulate the global distribution of internal-tidal energy, it is conceivable that the LNC may modulate the global ocean circulations and climate on a bidecadal timescale.

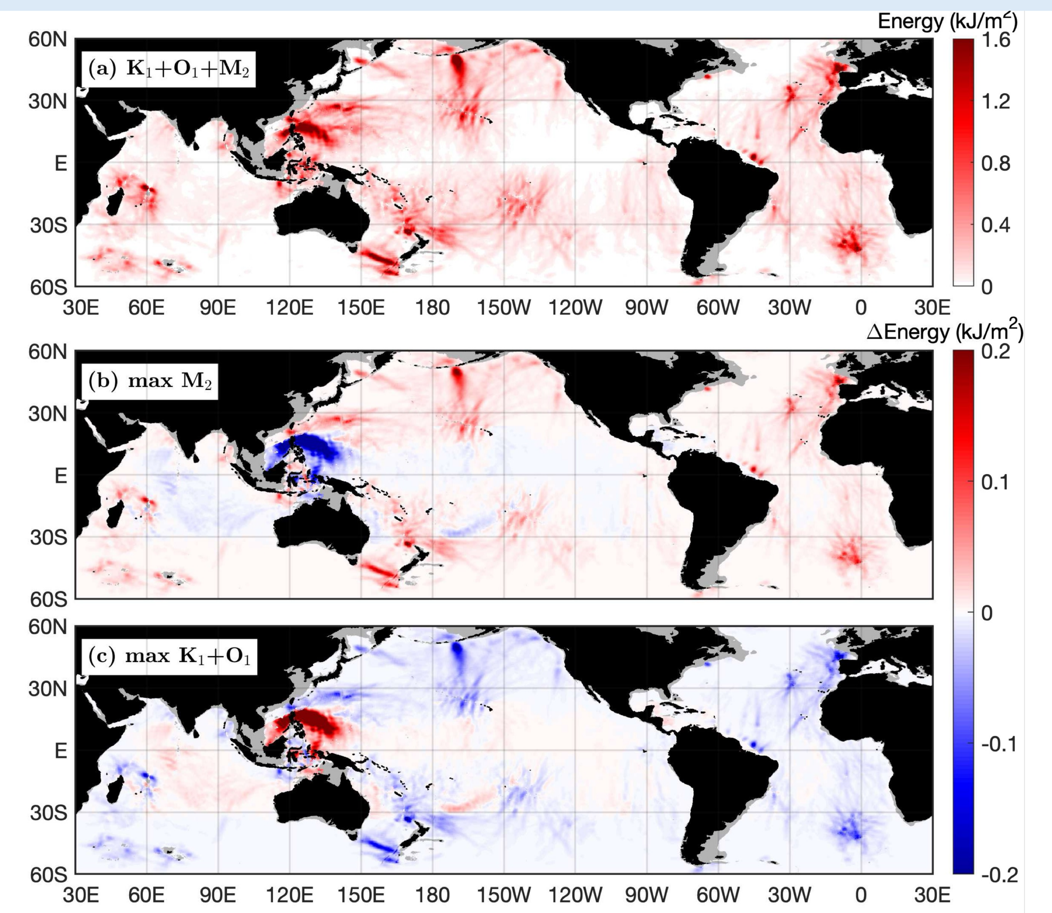

Figure 7. Spatial variation of internal tidal energy with the 18.6-year LNC. (a) Internal tidal energy (K_1+O_1+M_2). (b) Anomalous field at the time of maximal M_2. (c) Anomalous field at the time of maximal K_1 and O_1.

Conclusions

Both the 18.6-year LNC and long-term quasi-linear trends in oceanic internal tides are detected using 30 years of satellite altimeter data. Their global-mean amplitude and phase time series demonstrate that the detected LNC is consistent with the equilibrium theory. The detected quasi-linear trends are evidently the anticipated consequence of the increasingly stratified ocean caused by global warming. The global distribution of internal tidal energy is significantly modulated by the 18.6-year LNC. We suggest that the nodal modulation of internal tides may affect internal tide-driven ocean mixing and thus large-scale ocean circulations.